Article

Fractional Order, Interval Parameter, State Space Model of the One-Dimensional Heat Transfer Process

Krzysztof Oprzędkiewicz [*]

Article

Fractional Order, Interval Parameter, State Space Model of the One-Dimensional Heat Transfer Process

Krzysztof Oprzedkiewicz [ID]

AGH University, al. A. Mickiewicza 30, 30 -059 Kraków Poland; kop@agh.edu.pl

Abstract: In the paper the new, fractional order, state space model of a heat transfer in a one-dimensional metallic rod is addressed. The fractional orders of derivative along space and time are not exactly known and they are described by intervals. The proposed model is the interval expanding of the state space fractional model of the one dimensional heat transfer. It is expected to better describe the reality because interval order of each real process is hard to estimate. Elementary properties of the proposed model are analysed. Theoretical results are experimentally validated using data from real experimental laboratory system.

Keywords: fractional order systems; interval systems; heat transfer; state equation

---

1. Introduction

The modeling of processes and plants hard to describe using another mathematical tools is one of the main areas of application of the Fractional Order (FO) calculus.

Fractional order models of various physical phenomena have been presented by many Authors for years. Fundamental results are presented e.g. by [1], [2] (the heating of an one dimensional beam), [3] (FO models of chaotic systems and Ionic Polymer Metal Composites), [4]. FO models of diffusion processes are considered u.a. by [5] [6], and [7]. A collection of results using new Atangana-Baleanu operator can be found in [8]. This book presents i.e. the FO blood alcohol model, the Christov diffusion equation and fractional advection-dispersion equation for groundwater transport processes.

Recently FO models are used u.a. to describe a spread of diseases. As examples can be given the modeling of the dynamics of COVID using Caputo-Fabrizio operator presented by [9] or the model of transmission of Zika virus using Atangana-Baleanu operator is proposed by [10].

Models of temperature fields are considered by many Authors, e.g. [11] ,[12]. Analytical solution of the two-dimensional, IO heat transfer equation is presented in the paper [13]. Numerical methods of solution of PDE-s can be found, e.g., in [14]. Fractional Fourier integral operators are analyzed u.a. by [15]. It is important to note that a significant part of known investigations deals only with a steady-state temperature fields with omitting their dynamics.

The state space FO models of the one dimensional heat transfer have been proposed in many previous papers of author from years [16–23]. These models used different FO operators: Grünwald-Letnikov, Caputo, Caputo-Fabrizio and Atangana-Baleanu as well as discrete operators CFE and FOBD. Each proposed model has been thoroughly theoretically and experimentally verified. In addition, each of them assures better accuracy in the sense of square cost function than its IO analogue.

The sensitivity of the FO model to uncertainty of coefficients describing the heat conduction and heat exchange was analysed in the paper [24]. In this paper the uncertainty of fractional orders has not been considered. Such an analysis is given in this paper.

The papers [25] and [26] present the generalization of FO models mentioned above to the two dimensional case.

This article presents the generalization of the model given by [20] to the case when both fractional orders are described by intervals. Such an approach should better describe reality, because really the fractional orders are hard to estimate in contrast to parameters describing the heat transfer and heat conduction. From knowledge of author it turns out that such a model has not been proposed yet. The interval fractional order system was considered e.g. by [27], but this paper deals with the interval state operator and known interval order of derivative along the time.

The paper is organized as follows. Preliminaries recall some basic ideas from fractional calculus, necessary to present results. Next the experimental system and its FO model with interval orders is presented and analyzed. Finally theoretical results are validated using experiments.

2. Preliminaries

At the beginning the non integer order, integro-differential operator is presented (see e.g. [4], [28],[29], [1]).

Definition 1. *(The elementary non integer order operator) The non integer order integro-differential operator is defined as follows:*

$$
{}_aD_t^\alpha g(t) = \begin{cases} \frac{d^\alpha g(t)}{dt^\alpha} & \alpha > 0 \\ g(t) & \alpha = 0 \\ \int\limits_a^t g(\tau)(d\tau)^{-\alpha} & \alpha < 0 \end{cases} \quad .
\tag{1}
$$

where a and t denote time limits for operator calculation, $\alpha \in \mathbb{R}$ denotes the non integer order of the operation.

Next an idea of complete Gamma Euler function is recalled (see for example [29]):

Definition 2. *(The complete Gamma function)*

$$
\Gamma(x) = \int\limits_0^\infty t^{x-1}e^{-t}dt.
\tag{2}
$$

An idea of Mittag-Leffler function needs to be given next. It is a non integer order generalization of exponential function $e^{\lambda t}$ and it plays crucial role in the solution of a FO state equation. The two parameter Mittag-Leffler function is defined as follows:

Definition 3. *(The two parameter Mittag-Leffler function)*

$$
E_{\alpha,\beta}(x) = \sum_{k=0}^\infty \frac{x^k}{\Gamma(k\alpha + \beta)}.
\tag{3}
$$

For $\beta = 1$ we obtain the one parameter Mittag-Leffler function:

Definition 4. *(The one parameter Mittag-Leffler function)*

$$
E_\alpha(x) = \sum_{k=0}^\infty \frac{x^k}{\Gamma(k\alpha + 1)}.
\tag{4}
$$

The fractional order, integro-differential operator (1) can be expressed by three fundamental definitions, given by Grünwald and Letnikov (GL definition), Riemann and Liouville (RL definition) and Caputo (C definition). Relations between Caputo and Riemann-Liouville, between Riemann-Liouville and Grünwald-Letnikov operators are given e.g. in [30], [4]. Discrete versions of these operators are deeply analysed by [31]. The C definition has a simple interpretation of an initial

condition (it is analogical as in integer order case) and intuitive Laplace transform. Additionally its value from a constant equals to zero, in contrast to e.g. RL definition. That's why in the further consideration the C definition will be applied. It is recalled beneath.

Definition 5. *(The Caputo definition of the FO operator)*

$$
{}_{0}^{C}D_{t}^{\alpha}f(t) = \frac{1}{\Gamma(V-\alpha)} \int_{0}^{\infty} \frac{f^{(V)}(\tau)}{(t-\tau)^{\alpha+1-V}}d\tau.
\tag{5}
$$

In (5) V is a limiter of the non integer order: $V-1 \le \alpha < V$. If $V = 1$ then consequently $0 \le \alpha < 1$ is considered and the definition (5) takes the form:

$$
{}_{0}^{C}D_{t}^{\alpha}f(t) = \frac{1}{\Gamma(1-\alpha)} \int_{0}^{\infty} \frac{\dot{f}(\tau)}{(t-\tau)^{\alpha}}d\tau.
\tag{6}
$$

Finally a fractional linear state equation using Caputo definition needs to be recalled. It takes the following form:

$$
\begin{aligned}
{}_{0}^{C}D_{t}^{\alpha}x(t) &= Ax(t) + Bu(t) \\
y(t) &= Cx(t)
\end{aligned}
\tag{7}
$$

where $\alpha \in (0,1)$ is the fractional order of the state equation, $x(t) \in \mathbb{R}^{R}$, $u(t) \in \mathbb{R}^{L}$, $y(t) \in \mathbb{R}^{P}$ are the state, control and output vectors respectively, A, B, C are the state, control, and output matrices.

3. The Experimental System and Its Model with Fractional, Interval Orders

The experimental heat plant is shown in Figure 1. It has the form of a thin copper rod $260[mm]$ long. To simplify assume that its length equals to 1.0. This allows to express the localization and length of heater and RTD sensors with respect to 1.0. The rod is heated by the electric heater $\Delta x_0 = 0.14$ long located at the end of the rod. An output temperature is measured with the use of miniature RTD sensors (Pt100) long Δx attached in points: 0.29, 0.50 and 0.73 of rod length. The input signal of the system is the standard current from range $0 - 20[mA]$. It is amplified to the range $0 - 1.5[A]$ and it is the input signal for the heater. Signals from the RTD-s are read directly by analog input module in the PLC. Data from PLC are collected by SCADA application. The whole system is connected via PROFINET. The temeprature distribution with respect to time and length is shown in the Figure 2.
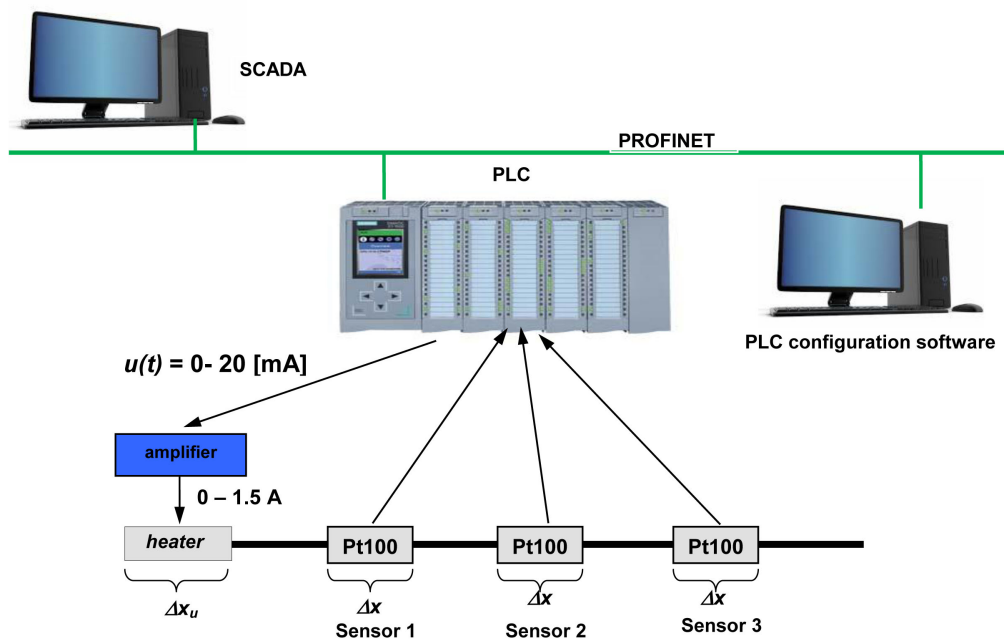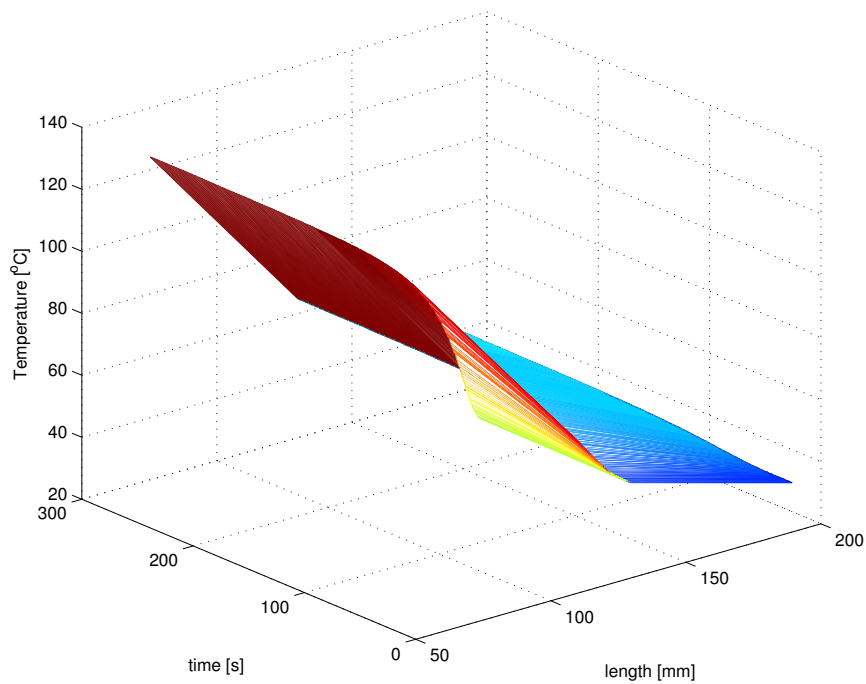
Figure 1. The experimental system

Figure 2. The spatial-time temperature distribution in the plant

The fundamental, time continuous model describing the heat conduction and dissipation in the rod is the partial differential equation of the parabolic type with the homogeneous Neumann boundary conditions at the ends, the homogeneous initial condition, the heat exchange along the length of rod and distributed control and observation. This equation with integer orders of both differentiations has been discussed in many papers, for example in [32–34].

The FO expanding of this model is presented with details in the papers [16,17]. In this paper its version with interval fractional order along the length is proposed. It takes the following form:

$$
\begin{cases}
{}^{C}D_t^{\alpha}Q(x,t) = a_w \dfrac{\partial^{\beta} Q(x,t)}{\partial x^{\beta}} - R_a Q(x,t) + b(x)u(t) \\
\dfrac{\partial Q(0,t)}{dx} = 0, t \geq 0 \\
\dfrac{\partial Q(1,t)}{dx} = 0, t \geq 0 \\
Q(x,0) = Q_0, 0 \leq x \leq 1 \\
y(t) = k_0 \int_0^1 Q(x,t)c(x)dx.
\end{cases}
\tag{8}
$$

In (8) a_w, R_a are known coefficients of heat conduction and heat exchange, k_0 is a steady-state gain.

The non integer orders α and β are not exactly known and they are described by the following intervals:

$$
\alpha = [\underline{\alpha}; \overline{\alpha}] \subset \mathbb{R}^+.
\tag{9}
$$

where:

$$
\begin{aligned}
\underline{\alpha} &= \alpha_o(1 - \delta), \\
\overline{\alpha} &= \alpha_o(1 + \delta).
\end{aligned}
\tag{10}
$$

where $0.0 < \delta < 1.0$. This deviation can be also expressed in percents: $0 < \delta < 100\%$

$$
\beta = [\underline{\beta}; \overline{\beta}] \subset \mathbb{R}^+.
\tag{11}
$$

where:

$$
\begin{aligned}
\underline{\beta} &= \beta_o(1 - \Delta), \\
\overline{\beta} &= \beta_o(1 + \Delta).
\end{aligned}
\tag{12}
$$

where $0.0 < \Delta < 1.0$ or equivalently $0 < \Delta < 100\%$.

The intervals α and β build the vector of uncertain orders q:

$$
q = [\alpha; \beta] \subset \mathbb{I}(\mathbb{R}^2).
\tag{13}
$$

All the vectors q build the space of uncertain orders Q:

$$
Q = \{q = q = [\alpha; \beta] : \ \underline{\alpha} \leq \alpha \leq \overline{\alpha}, \ \underline{\beta} \leq \beta \leq \overline{\beta}\}.
\tag{14}
$$

The set Q can be interpreted as the rectangle in the $\mathbb{R}^2$ plane stretched on the following vertices:

$$
\begin{aligned}
q_{ll} &= \left[\underline{\alpha}, \underline{\beta}\right], \\
q_{lh} &= \left[\underline{\alpha}, \overline{\beta}\right], \\
q_{hl} &= \left[\overline{\alpha}, \underline{\beta}\right], \\
q_{hh} &= \left[\overline{\alpha}, \overline{\beta}\right].
\end{aligned}
\tag{15}
$$

The center of the rectangle Q is defined by the nominal values of orders:

$$
q_o = [\alpha_o, \beta_o].
\tag{16}
$$

The interval form of orders α and β expands the heat transfer equation (8) to the infinite set of equations, limited by vertices (15).

The differential equation (8) can be expressed as beneath:

$$\begin{cases} {}^{C}D_t^{\alpha}Q(t) = AQ(t) + Bu(t) \\ Q(0) = Q_0 \\ y(t) = k_0 C Q(t) \end{cases} \tag{17}$$

where:

$$\begin{cases} AQ = a_w \dfrac{\partial^{\beta} Q(x)}{\partial x^{\beta}} - R_a Q, \\ \mathcal{D}(A) = \{Q \in H^2(0,1) : Q'(0) = 0, Q'(1) = 0\}, \\ a_w, R_a > 0, \\ H^2(0,1) = \{u \in L^2(0,1) : u', u'' \in L^2(0,1)\}, \\ CQ(t) = \langle c, Q(t) \rangle, \ Bu(t) = \langle bu(t) \rangle \\ Q(t) = [q_1(t), q_2(t)..]^T. \end{cases} \tag{18}$$

In (18) $\mathcal{D}(A)$ denotes the field of the state operator A, $'$, $''$ denotes the first and second derivative along the length, $< .. >$ is the standard scalar product.

The basis of the state space is spanned by eigenvectors of the state operator A:

$$h_n = \begin{cases} 1, n = 0 \\ \sqrt{2}cos(n\pi x), n = 1, 2, ... \end{cases}. \tag{19}$$

3.1. The Decomposition of the Spectrum

The eigenvalues of the state operator A depend only on interval order β:

$$\lambda_n(\beta) = -a_w(n\pi)^{\beta} - R_a, \ n = 0, 1, 2, ... \tag{20}$$

and consequently for the interval β_I each eigenvalue expands to the interval too:

$$\lambda_{In} = \left[\lambda_n(\underline{\beta}); \lambda_n(\overline{\beta}) \right]. \tag{21}$$

Consequently the diagonal state operator has interval, diagonal form:

$$A_I = diag\{\lambda_{I0}, \lambda_{I1}, \lambda_{I2}, ...\}. \tag{22}$$

The spectrum σ of the state operator A is a set of all its eigenvalues:

$$\sigma(A_I) = \{\lambda_{I0}, \lambda_{I1}, \lambda_{I2}, ...\}. \tag{23}$$

For exactly known β the spectrum contains negative, real, single, separated eigenvalues ordered by indices n: $\lambda_0 > \lambda_1 > \lambda_2....$ The most poorly damped eigenvalue λ_0 is called the dominant (leading) eigenvalue. This property allows to easily decompose a system into single, scalar subsystems associated to particular eigenvalues. This is presented with details by [16], [17].

However for interval β_I situation gets more complicated due to particular eigenvalues expand to intervals. This implies that eigenvalues associated to different modes can partially overlap. In such a situation the spectrum decomposition is impossible because there exist two or more different, indistinguishable eigenvalues. This situation is illustrated by the Figure 3.
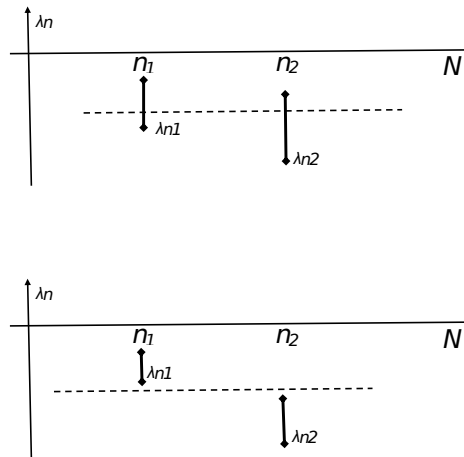
Figure 3. The part of specrum with eigenvalues λ_{n1} and λ_{n2}: overlapped in the top and non overlapped in the bottom.

The above situation can occur if the interval β_I is too wide. Simultaneously, narrow range of uncertainty guarantees the distinguishability of the spectrum. The maximum values of Δ_d and Δ_a assuring the distinguishability are described by the following Propositions.

Proposition 1. *(The maximum size of Δ_d assuring the distinguishability of any two eigenvalues) Consider the interval spectrum* (23) *of the system* (17). *Assume that the relative uncertainty of the order β is equal Δ.*

The size Δ_d assuring the distinguishability of two eigenvalues n_1 and n_2 is expressed by the following inequality:

$$\Delta_d \le \frac{L-1}{L+1}, \tag{24}$$

where:

$$L = \frac{\ln(n_2\pi)}{\ln(n_1\pi)}. \tag{25}$$

Proposition 2. *(The maximum size of Δ_a assuring the distinguishability of two adjacent eigenvalues) Consider the interval spectrum* (23) *of the system* (17). *Assume that the relative uncertainty of the order β is equal Δ.*

The size Δ_a assuring the distinguishability of the two adjacent eigenvalues n and $n+1$ is expressed by the following inequality:

$$\Delta_a \le \frac{L_a-1}{L_a+1}, \tag{26}$$

where:

$$L_a = \frac{\ln(n\pi)}{\ln((n+1)\pi)}. \tag{27}$$

The proof of both propositions is given beneath.

Proof. Consider two different interval eigenvalues and denote they by n_1 and n_2. Assume that they are partially overlapped. This is expressed as follows:

$$\begin{aligned}
&\lambda_{n_1}(\overline{\beta}) \ge \lambda_{n_2}(\underline{\beta}) \iff \\
&-a_w(n_1\pi)^{\beta+\Delta\beta} - R_a \ge -a_w(n_2\pi)^{\beta-\Delta\beta} - R_a \iff \\
&(n_1\pi)^{\beta(1+\Delta)} \ge (n_2\pi)^{\beta(1-\Delta)}.
\end{aligned} \tag{28}$$

Using logarithm function we obtain:

$$\beta(1+\Delta)\ln(n_1\pi \ge \beta(1-\Delta)\ln(n_2\pi). \tag{29}$$

After some elementary transformations we obtain (24) and the proof is completed. Assuming $n_1 = n$ and $n_2 = n + 1$ gives directly condition (26). $\square$

It is important to note that the maximum uncertainty permitted from point of view of spectrum decomposition does not depend on the value of β and it is determined only by location of eigenvalues, described by their indices.

Using the condition (24) the maximum order N assuring the distinguishability of all eigenvalues for given uncertainty Δ can be given too. It is described by the following proposition.

Proposition 3. *(The maximum dimension of the model N guaranteeing the distinguishability of the spectrum)*

Consider the interval spectrum (23) of the system (17). Assume that the relative uncertainty of the order β is equal Δ.

The maximum size N of the model assuring the distinguishability of all eigenvalues meets the following inequality:

$$\frac{N}{(N-1)^D} \geq \pi^{D-1}, \tag{30}$$

where:

$$D = \frac{1+\Delta}{1-\Delta}. \tag{31}$$

Proof. Computing L from (24) we obtain:

$$L \geq D$$

Assuming $n_2 = N$ and $n_1 = N - 1$ in (25) yields:

$$
\begin{aligned}
\ln(n) + \ln(\pi) &\geq D\ln(N-1) + D\ln(\pi) \iff \\
\ln(N) - D(\ln(N-1)) &\geq (D-1)\ln(\pi) \iff \\
\ln\left(\frac{N}{(N-1)^D}\right) &\geq \ln\left(\pi^{(D-1)}\right).
\end{aligned}
\tag{32}
$$

From (32) we obtain (30) and the proof is completed. $\square$

The dependence (30) gives the implicit condition to estimate N. However it can be easily applied numerically. This will be shown in the section "Simulations".

3.2. The Input and Output Operators

Next recall the form of input and output operators, presented e.g. in [35]. They do not depend on interval orders of the system.

The input operator B describes the location and construction of heater. It is as follows:

$$B = [b_0, b_1, b_2, ...]^T. \tag{33}$$

where $b_n = \langle b, h_n \rangle$, $b(x)$ is the shaping function of the heater:

$$b(x) = \begin{cases} 1, x \in [0, x_u] \\ 0, x \notin [0, x_u] \end{cases}. \tag{34}$$

According to (19) and (34) each element b_n takes the following form:

$$b_n = \begin{cases} x_u, \ n = 0, \\ \frac{\sqrt{2}sin(n\pi x_u)}{n\pi}, \ n = 1, 2, ... \end{cases}. \tag{35}$$

The output operator C describes the location and size of RTD-s. It is as beneath:

$$C = [c_0, c_1, c_2, \ldots]. \tag{36}$$

In (36) $c_n = \langle c, h_n \rangle$, $c(x)$ is the output sensor function:

$$c(x) = \begin{cases} 1, x \in [x_1, x_2] \\ 0, x \notin [x_1, x_2] \end{cases}. \tag{37}$$

Using (19) and (37) yields:

$$c_n = \begin{cases} x_2 - x_1, \; n = 0, \\ \frac{\sqrt{2}(sin(n\pi x_2) - sin(n\pi x_1))}{n\pi}, \; n = 1, 2, \ldots \end{cases} \tag{38}$$

It is important to note that the operators B and C do not depend on the uncertain orders α and β.

The shaping function $b(x)$ and sensor function $c(x)$ are piecevise constant functions.

3.3. The Step and Impulse Responses of the System with Interval Orders

If the control is the Heaviside function: $u(t) = 1(t)$ then the analytical formula of step response is as beneath:

$$y_\infty(t) = \sum_{n=0}^{\infty} \frac{(E_\alpha(\lambda_n t^\alpha) - 1(t))}{\lambda_n} b_n c_n. \tag{39}$$

where E_α is the one parameter Mittag-Leffler function, λ_n, b_n and c_n are expressed by (20), (35) and (38) respectively. Analogically we can compute the impulse response:

$$g_\infty(t) = \sum_{n=0}^{\infty} c_n b_n t^{\alpha-1} E_{\alpha,\alpha}(\lambda_n t^\alpha). \tag{40}$$

In (40) $E_{\alpha,\alpha}$ is two parameter Mittag-Leffler function.

The non integer order model described by (17) - (40) is infinite dimensional. It is obvious that its practical use requires its reduction to finite dimensional form. This can be done by truncating further modes in state equation (17) and computing solution (39) or (40) as a finite sum. Consequently operators A, B and C reduce to matrices as well as the both time responses take the form of finite sums:

$$y(t) = y_0 \sum_{n=1}^{N} \frac{(E_\alpha(\lambda_{In} t^\alpha) - 1(t))}{\lambda_{In}} b_n c_n. \tag{41}$$

$$g(t) = \sum_{n=0}^{N} c_n b_n t^{\alpha-1} E_{\alpha,\alpha}(\lambda_{In} t^\alpha). \tag{42}$$

In (41) and (42) N is the order of finite approximation. Its value determines the accuracy of the model. It can be estimated using numerical or analytical methods (see [17]).

The time responses (41) and (42) are functions of interval orders collected in the vectors (13): $y(t) = y(t, q)$, $g(t) = g(t, q)$. This expands they to sectors limited by the borders of intervals α and β:

$$\begin{aligned} y_{ll}(t) &= y(t, q_{ll}), \\ y_{lh}(t) &= y(t, q_{lh}), \\ y_{hl}(t) &= y(t, q_{hl}), \\ y_{hh}(t) &= y(t, q_{hh}). \end{aligned} \tag{43}$$

$$
\begin{aligned}
g_{ll}(t) &= g(t, q_{ll}), \\
g_{lh}(t) &= g(t, q_{lh}), \\
g_{hl}(t) &= g(t, q_{hl}), \\
g_{hh}(t) &= g(t, q_{hh}).
\end{aligned}
\tag{44}
$$

In (43) and (44) $q_{..}$ are defined by (15). Analogically the nominal time responses are expressed as follows:

$$
y_o(t) = y(t, q_o),
\tag{45}
$$

$$
g_o(t) = g(t, q_o).
\tag{46}
$$

where q_o is the vector of nominal parameters (16).

The most obvious way to describe the sensitivity of the step response $y(t)$ to uncertainty of the orders α is to propose the sensitivity functions in the form $\frac{\partial y(t)}{\partial \delta}$ and $\frac{\partial y(t)}{\partial \Delta}$. However such explicit functions are hard to compute.

The sensitivity can be also tested using the following relative dynamic deviations $E_{..}(t)$:

$$
E_{..}(t) = \frac{e_{..}(t)}{y_o(t)} \cdot 100\%.
\tag{47}
$$

where $_{..} = {}_{ll, \ lh, \ hl, \ hh}$ and:

$$
\begin{aligned}
e_{ll}(t) &= |y_o(t) - y_{ll}(t)|, \\
e_{lh}(t) &= |y_o(t) - y_{lh}(t)|, \\
e_{hl}(t) &= |y_o(t) - y_{hl}(t)|, \\
e_{hh}(t) &= |y_o(t) - y_{hh}(t)|.
\end{aligned}
\tag{48}
$$

3.4. The Steady-State Response

The steady-state response of the system is as follows:

$$
y_N^{ss}(\beta) = \sum_{n=0}^{N} y_n^{ss}(\beta),
\tag{49}
$$

where y_n^{ss} are expressed as follows:

$$
y_n^{ss}(\beta) = \frac{b_n c_n}{a_w (n\pi)^\beta + R_a},
\tag{50}
$$

in (50) b_n and c_n are described by (35) and (38) respectively.

The responses y_n^{ss} do not depend on the order α, but they are affected by the interval order β only. From the point of view of the geometric interpretation the rectangle (14), (15) reduces to the section limited by the limits of the order β. This is expressed as beneath:

$$
\begin{aligned}
\lim_{t \to \infty} y_{nll}(t) &= \lim_{t \to \infty} y_{nhl}(t) = y_{nl}^{ss}, \\
\lim_{t \to \infty} y_{nlh}(t) &= \lim_{t \to \infty} y_{nhh}(t) = y_{nh}^{ss}.
\end{aligned}
\tag{51}
$$

where nominal and limit values re described a s follows:

$$
\begin{aligned}
y_{nl}^{ss} &= y_n^{ss}(\overline{\beta}), \\
y_{no}^{ss} &= y^{ss}(\beta_o), \\
y_{nh}^{ss} &= y_n^{ss}(\underline{\beta}).
\end{aligned}
\tag{52}
$$

and consequently the whole response (49) takes the form of the following interval:

$$y_{Nh,o,l}^{ss} = \sum_{n=0}^{N} y_{nh,o,l}^{ss}. \tag{53}$$

The relative deviation E^{ss} of the steady-state response from its nominal value is the limit value of deviation $E_{..}(t)$ expressed by (47):

$$E_{l,h}^{ss} = \lim_{t\to\infty} E_{ll,hl,lh,hh}(t). \tag{54}$$

Using (53) the deviation (54) is expressed as:

$$E_{l,h}^{ss} = \frac{|y_{No}^{ss} - y_{Nl,h}^{ss}|}{y_{No}^{ss}} \cdot 100\%. \tag{55}$$

4. Experiments and Simulations

The experiments were done using the system presented in the section I. The experimental step response was realized by change of input signal from 40% to 60% of its maximum range. The time-spatial temperature distribution is shown in the Figure 2. During experiments the sample time was equal: $h = 1[s]$, the number of samples was equal: $K_s = 300$ and the final time was equal: $t_f = 300[s]$. The size and location of heater and sensors are given in the Table 1.

Table 1. The size and the location of the heater and the sensors

Δx_u	Δx	x_1	x_2	x_3
0.14	0.06	0.26	0.47	0.70

The analysis of sensitivity was done using parameters of the model estimated numerically via minimization of the MSE cost function for all sensors together (see [17]- caption of the Fig. 6). These parameters are recalled in the Table 2. The values of α and β are set as the nominal values α_o and β_o.

Table 2. The parameters of the model

α_o	β_o	a_w	R_a	N
0.930289	1.998808	0.000410	0.0677066	22

The impact of uncertainties δ and Δ to model was examined numerically. Results are presented in the next subsections.

### 4.1. The Analysis of the Spectrum Decomposition

At the beginning the impact of the uncertainty Δ to spectrum decomposition was tested using conditions (24), (26) and (30).

The general condition (24) was examined for indices n_1 and n_2 describing rather distant eigenvalues. Results are completed in the Table 3.

Table 3. The maximum size Δ_d allowing to distinguish two different eigenvalues

n_1	n_2	Δ_d
2	10	0.3045
2	30	0.4242
5	20	0.2011
10	25	0.1173
15	25	0.0622
20	25	0.0262
25	30	0.0205

Next the distinguishability of adjacent eigenvalues was tested using condition (26). Results are illustrated by the Figure 4.
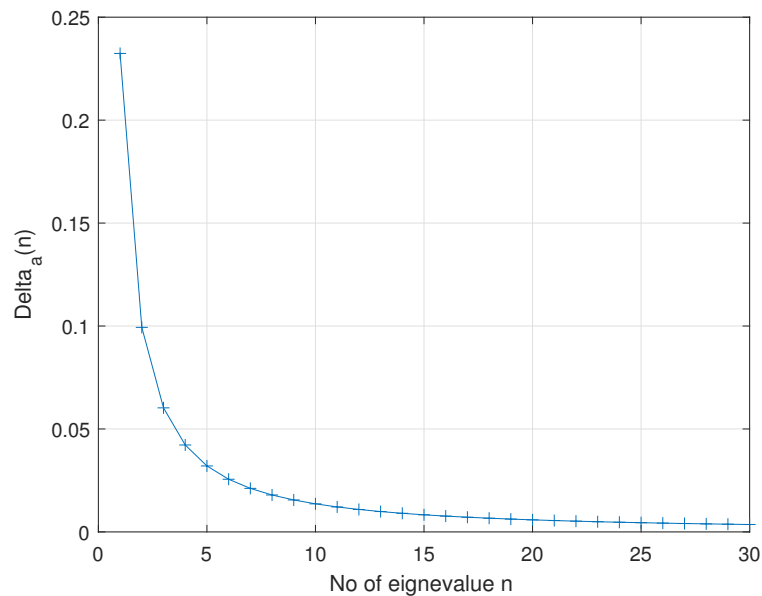
Figure 4. The maximum uncertainty Δ_a assuring the distinguishability of two adjacent eigenvalues.

The Table 3 and Figure 4 show that the distinguishability is harder to keep for "further" eigenvalues with higher indices n.

Finally the maximum order N assuring the distinguishability of the whole spectrum was computed using condition (30). To make it easier denote the left and right side of inequality (30) by f_1 and f_2:

$$f_1(N, \Delta) = \frac{N}{(N-1)^D},$$
$$f_2(N, \Delta) = \pi^{D-1}. \tag{56}$$

Using this notation the condition (30) turns to the following form:

$$f_1(N, \Delta) \leq f_2(N, \Delta). \tag{57}$$

The condition (57) was tested numerically for $\Delta = 0.01$ and $\Delta = 0.005$. Numerical solution of the inequality (57) is shown in the Figure 5.
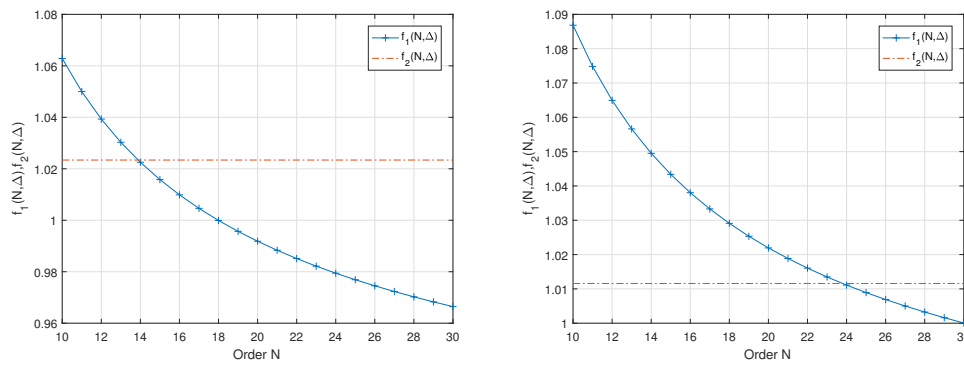
Figure 5. The maximum N assuring the distinguishability of all eigenvalues for $\Delta = 0.01$ (left) and $\Delta = 0.005$ (right).

The diagrams in the Figure 5 show that for $\Delta = 0.01$ the maximum size of model is equal 13 and for $\Delta = 0.005$ this maximum size is equal 23. In general, the increasing of the uncertainty Δ causes the decreasing of the order of the model N assuring the distinguishability of the spectrum.

4.2. The Sensitivity of the Dynamics

The sensitivity of the step response to uncertainties of both orders was tested using dynamic relative deviations (47) computed using data from the table 2. Both uncertainties was set to: $\delta = 0.01 = 1\%$ and $\Delta = 0.01 = 1\%$. All vertex step responses for all outputs are compared to nominal one and experimental in the Figure 6. Time trends of all deviations for all outputs of the system $E_{..}(t)$ are shown in the Figure 7.
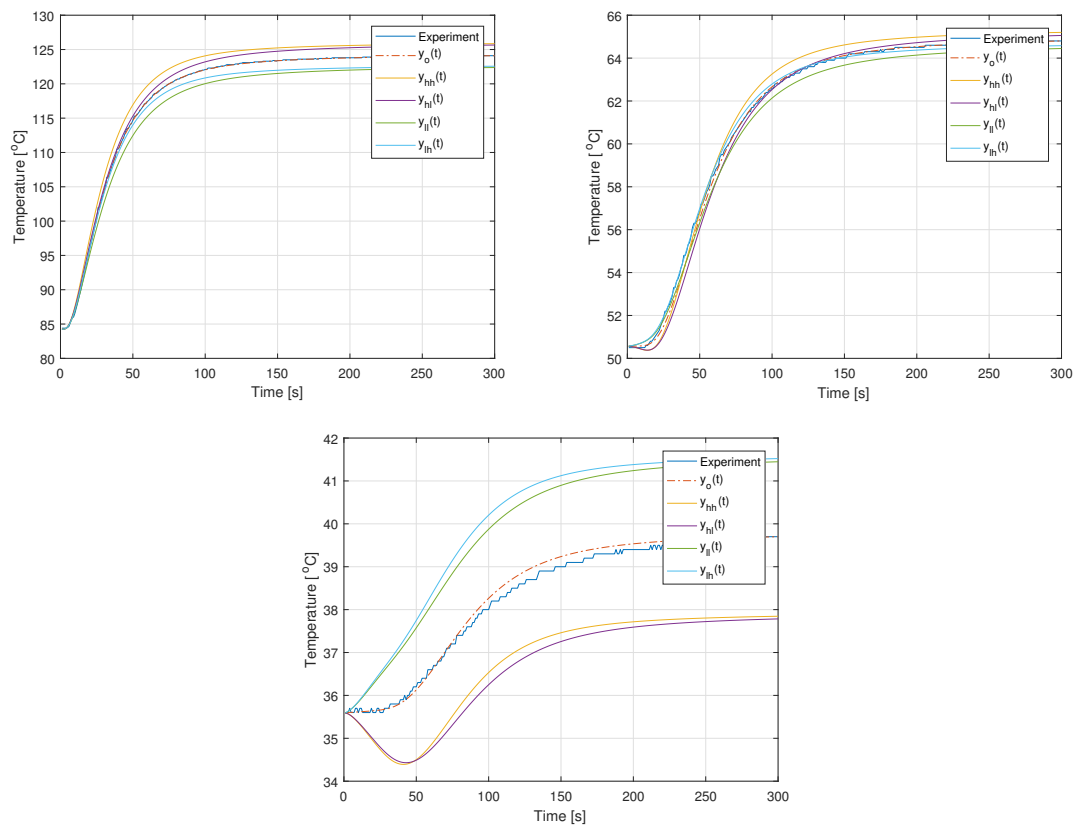
Figure 6. The vertex step responses (43) of the model for $\delta = 0.01$ and $\Delta = 0.01$ for outputs 1-3 (1-top, 3-bottom)
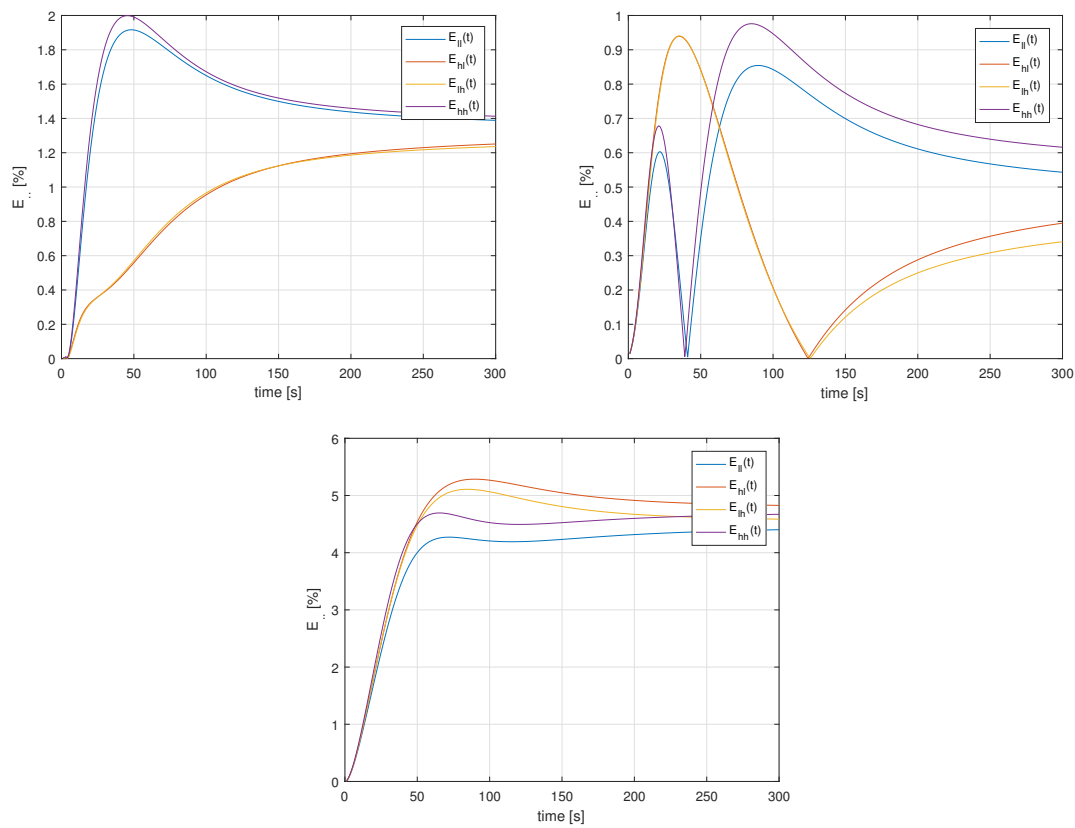
Figure 7. The relative deviations (47) for $\delta = 1\%$ and $\Delta = 1\%$ for outputs 1-3 (1-top, 3-bottom).

In diagrams 6 and 7 it can be noted that the shape and maximum of deviation (47) strongly depends on the observed output. It is smallest for sensor no 2 and biggest for sensor no 3. Next, the impact of the uncertainty δ goes to zero for $t \to \infty$.
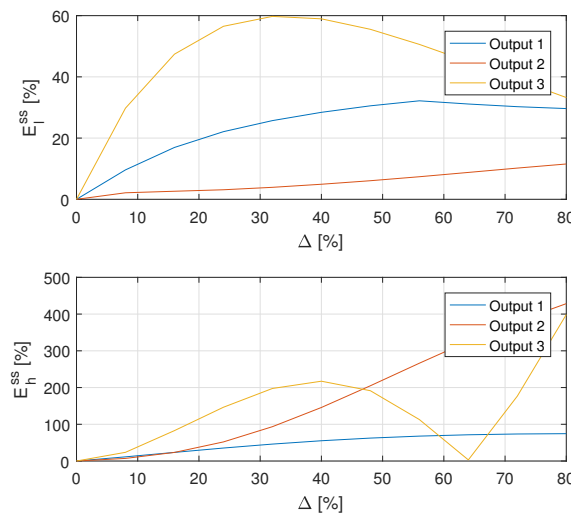
4.3. The Sensitivity of the Steady-State Response

The relative steady-state error (55) was examined for small uncertainty included in the range $0\% < \Delta < 2\%$ and big uncertainty from range $0\% < \Delta < 80\%$ separately. Results are illustrated by Figures 8 and 9.
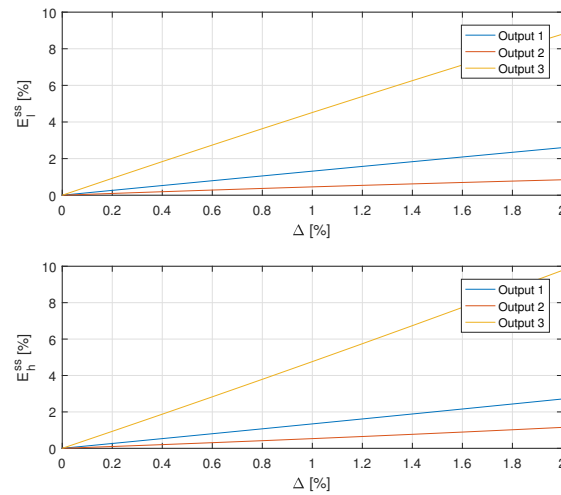
Figure 8. The relative steady-state deviation (55) as a function of the small uncertainty $0\% < \Delta < 2\%$ for all outputs of the plant.

Figure 9. The relative steady-state deviation (55) as a function of the big uncertainty $0\% < \Delta < 80\%$ for all outputs of the plant.

The analysis of diagrams 8 and 9 allows to conclude that:

- The sensitivity of the steady-state response to uncertainty Δ strongly depends on the localisation of the RTD. Its is highest for the most distant sensor 3 and smaller for sensors 1 and 2.
- For small uncertainty the deviation E^{ss} is approximately a linear function of Δ and both deviations $E^{ss}_{h,l}$ are approximately the same.
- For bigger uncertainty the deviation E^{ss} is a nonlinear function of Δ and nonlinearity is variuos for different outputs. Additionally, the upper deviation E^{ss}_h is much bigger than lower E^{ss}_l.

5. Final Conclusions

The results presented in the paper can be summarized that the uncertainty of both fractional orders impacts to crucial properties of the model: the distinguishability of the spectrum, the step and steady-state responses. The disturbation of order α affects only to dynamics, but the disturbation of the order β expressed by Δ disturbs all considered properties of the model.

Next, the impact of the disturbation Δ is determined by its size and the place of measurement. Small disturbation (circa 1%) strongly disturbs the output 3 furthest from the heater and slightly interferes with the measurement at output 2, placed halfway along the length of the rod. In turn, a large disturbance (greater than 50%) disturbs output 1 the least.

Further research of the presented issues will include among others theoretical justification of numerical results and investigation of discrete, approximated models using CFE and FOBD approximations.

6. Acknowledgment

References

1. Podlubny, I. *Fractional Differential Equations*; Academic Press: San Diego, 1999.
2. Dzieliński, A.; Sierociuk, D.; Sarwas, G. Some applications of fractional order calculus. *Bulletin of the Polish Academy of Sciences, Technical Sciences* **2010**, *58*, 583–592.
3. Caponetto, R.; Dongola, G.; Fortuna, L.; Petras, I. Fractional Order Systems: Modeling and Control Applications. In *World Scientific Series on Nonlinear Science*; Chua, L.O., Ed.; University of California: Berkeley, 2010; pp. 1–178.
4. Das, S. *Functional Fractional Calculus for System Identification and Controls*; Springer: Berlin, 2010.
5. Gal, C.; Warma, M. Elliptic and parabolic equations with fractional diffusion and dynamic boundary conditions. *Evolution Equations and Control Theory* **2016**, *5*, 61–103.
6. Popescu, E. On the fractional Cauchy problem associated with a Feller semigroup. *Mathematical Reports* **2010**, *12*, 181–188.
7. Sierociuk, D.; Skovranek, T.; Macias, M.; Podlubny, I.; Petras, I.; Dzielinski, A.; Ziubinski, P. Diffusion process modeling by using fractional-order models. *Applied Mathematics and Computation* **2015**, *257*, 2–11.
8. Gómez, J.F.; Torres, L.; (Eds), R.E. Fractional Derivatives with Mittag-Leffler Kernel. Trends and Applications in Science and Engineering. In *Studies in Systems, Decision and Control, vol. 194*; Kacprzyk, J., Ed.; Springer: Switzerland, 2019; pp. 1–339.
9. A., B.; hadj Moussa Y., E.; Hammouch.; S., U. A fractional-order model describing the dynamics of the novel coronavirus (COVID-19) with nonsingular kernel. *Chaos, Solitons and Fractals* **2021**, *146*, 1–11.
10. M., F.; A., A.; S., A.; T., B.; A., A.; H., A. Modeling and analysis of fractional order Zika model. *AIMS Mathematics* **2022**, *7*, 3912–3938.
11. Dlugosz, M.; Skruch, P. The application of fractional-order models for thermal process modelling inside buildings. *Journal of Building Physics* **2015**, *1*, 1–13.
12. Ryms, M.; Tesch, K.; Lewandowski, W. The use of thermal imaging camera to estimate velocity profiles based on temperature distribution in a free convection boundary layer. *International Journal of Heat and Mass Transfer* **2021**, *165*, 120686.
13. Khan, H.; Shah, R.; Kumam, P.; Arif, M. Analytical Solutions of Fractional-Order Heat and Wave Equations by the Natural Transform Decomposition Method. *Entropy* **2019**, *21*, 597–618.
14. Olsen-Kettle, L. *Numerical solution of partial differential equations*; The University of Queensland: Queensland, Australia, 2011.
15. Al-Omari, S.K. A fractional Fourier integral operator and its extension to classes of function spaces. *Advances in Difference Equations* **2018**, *1*, 1–9.
16. Oprzędkiewicz, K.; Gawin, E.; Mitkowski, W. Modeling heat distribution with the use of a non-integer order, state space model. *International Journal of Applied Mathematics and Computer Science* **2016**, *26*, 749–756.

17. Oprzędkiewicz, K.; Gawin, E.; Mitkowski, W. Parameter identification for non integer order, state space models of heat plant. In Proceedings of the MMAR 2016 : 21th international conference on Methods and Models in Automation and Robotics : 29 August–01 September 2016, Międzyzdroje, Poland, 2016, pp. 184–188.

18. Oprzedkiewicz, K.; Stanislawski, R.; Gawin, E.; Mitkowski, W. A new algorithm for a CFE approximated solution of a discrete-time non integer-order state equation. *Bulletin of the Polish Academy of Sciences. Technical Sciences* **2017**, *65*, 429–437.

19. Oprzędkiewicz, K.; Mitkowski, W.; Gawin, E. An accuracy estimation for a non integer order, discrete, state space model of heat transfer process. In Proceedings of the Automation 2017 : innovations in automation, robotics and measurment techniques : 15-17 March, Warsaw, Poland, 2017, pp. 86–98.

20. Oprzędkiewicz, K.; Mitkowski, W.; Gawin, E.; Dziedzic, K. The Caputo vs. Caputo-Fabrizio operators in modeling of heat transfer process. *Bulletin of the Polish Academy of Sciences. Technical Sciences* **2018**, *66*, 501–507.

21. Oprzędkiewicz, K.; Gawin, E. The practical stability of the discrete, fractional order, state space model of the heat transfer process. *Archives of Control Sciences* **2018**, *28*, 463–482.

22. Oprzędkiewicz, K.; Mitkowski, W. A memory efficient non integer order discrete time state space model of a heat transfer process. *International Journal of Applied Mathematics and Computer Science* **2018**, *28*, 649–659.

23. Oprzędkiewicz, K. Non integer order, state space model of heat transfer process using Atangana-Baleanu operator. *Bulletin of the Polish Academy of Sciences. Technical Sciences* **2020**, *68*, 43–50.

24. Oprzędkiewicz, K. Fractional order, discrete model of heat transfer process using time and spatial Grünwald-Letnikov operator. *Bulletin of the Polish Academy of Sciences. Technical Sciences* **2021**, *69*, 1–10.

25. Oprzędkiewicz, K.; Mitkowski, W.; Rosol, M. Fractional order model of the two dimensional heat transfer process. *Energies* **2021**, *14*, 1–17.

26. Oprzędkiewicz, K.; Mitkowski, W.; Rosol, M. Fractional order, state space model of the temperature field in the PCB plate. *Acta Mechanica et Automatica* **2023**, *17*, 180–187.

27. Kaczorek, T. Stability of interval positive fractional discrete-time systems. *International Journal of Applied Mathematics and Computer Science* **2018**, *28*, 451–456.

28. Kaczorek, T. Singular fractional linear systems and electrical circuits. *International Journal of Applied Mathematics and Computer Science* **2011**, *21*, 379–384.

29. Kaczorek, T.; Rogowski, K. *Fractional Linear Systems and Electrical Circuits*; Bialystok University of Technology: Bialystok, 2014.

30. Bandyopadhyay, B.; Kamal, S. Solution, Stability and Realization of Fractional Order Differential Equation. In *Stabilization and Control of Fractional Order Systems: A Sliding Mode Approach, Lecture Notes in Electrical Engineering 317*; Springer: Switzerland, 2015; pp. 55–90.

31. D., M.; E., G.; M., W. Comparison of h-difference fractional operators. In *Advances in the Theory and Applications of Non-integer Order Systems*; et al, W.M., Ed.; Springer: Switzerland, 2013; pp. 1–178.

32. Oprzędkiewicz, K. The interval parabolic system. *Archives of Control Sciences* **2003**, *13*, 415–430.

33. Oprzędkiewicz, K. A controllability problem for a class of uncertain parameters linear dynamic systems. *Archives of Control Sciences* **2004**, *14*, 85–100.

34. Oprzędkiewicz, K. An observability problem for a class of uncertain-parameter linear dynamic systems. *International Journal of Applied Mathematics and Computer Science* **2005**, *15*, 331–338.

35. Oprzędkiewicz, K. Positivity problem for the one dimensional heat transfer process. *ISA Transactions* **2021**, *112*, 281–291.